Neoplasia • Vol. 9, No. 8, August 2007, pp. 643–651 643

www.neoplasia.com

Expression and Function of the Human Androgen-Responsive Gene *ADI1* in Prostate Cancer[1]

Shane W. Oram, Junkui Ai[†,2,3], Gina M. Pagani[‡,2], Moira R. Hitchens[†], Jeffrey A. Stern*, Scott Eggener*, Michael Pins*, Wuhan Xiao*, Xiaoyan Cai*, Riffat Haleem*, Feng Jiang*, Thomas C. Pochapsky[‡,§], Lizbeth Hedstrom[‡,§] and Zhou Wang*[,†]*

*Department of Urology, Feinberg School of Medicine, Northwestern University, Chicago, IL 60611, USA; [†]Department of Urology, University of Pittsburgh School of Medicine, University of Pittsburgh Cancer Institute, University of Pittsburgh Medical Center, Pittsburgh, PA 15232, USA; [‡]Department of Biochemistry, Brandeis University, Waltham, MA 02454, USA; [§]Department of Chemistry, Brandeis University, Waltham, MA 02454, USA

Abstract

We have previously identified an androgen-responsive gene in rat prostate that shares homology with the aci-reductone dioxygenase (ARD/ARD′) family of metal-binding enzymes involved in methionine salvage. We found that the gene, aci-reductone dioxygenase 1 (*ADI1*), was downregulated in prostate cancer cells, whereas enforced expression of rat *Adi1* in these cells caused apoptosis. Here we report the characterization of human *ADI1* in prostate cancer. Androgens induced *ADI1* expression in human prostate cancer LNCaP cells, which was not blocked by cycloheximide, indicating that *ADI1* is a primary androgen-responsive gene. In human benign prostatic hyperplasia specimens, epithelial cells expressed *ADI1*. Immunohistochemistry of prostate tumor tissue microarrays showed that benign regions expressed more ADI1 than tumors, suggesting a suppressive role for ADI1 in prostate cancer. Bacterial lysates containing recombinant ADI1 produced a five-fold increase in aci-reductone decay over controls, demonstrating that ADI1 has ARD activity. We generated point mutations at key residues in the metal-binding site of *ADI1* to disrupt ARD function, and we found that these mutations did not affect intracellular localization, apoptosis, or colony formation suppression in human prostate cancer cells. Collectively, these observations argue that ADI1 may check prostate cancer progression through apoptosis and that this activity does not require metal binding.

Neoplasia (2007) **9,** 643–651

Keywords: *ADI1*, androgen-responsive gene, prostate cancer, aci-reductone dioxygenase, apoptosis.

Introduction

Prostate cancer remains the most frequently diagnosed cancer and second leading cause of cancer-related deaths in American men [1]. As androgens are intimately associated with disease progression, elucidating the roles and mechanisms of androgen action in prostate cancer is relevant to the prevention and treatment of the disease [2–4]. Androgen action is mediated through the androgen receptor, a ligand-dependent transcription factor that regulates the expression of androgen-responsive genes [5,6]. Thus, the identification and characterization of androgen-responsive genes in the prostate will likely provide insights into the mechanism by which androgens influence prostate cancer progression.

We have previously identified and characterized a rat androgen-responsive gene that encodes a 179–amino acid polypeptide with high homology to the ARD/ARD′ family [7]. We initially designated this gene as aci-reductone dioxygenase-like protein-1 (*ALP-1*), but to correspond with the official gene nomenclature, we have since renamed it aci-reductone dioxygenase-1. The ARD/ARD′ family, first discovered in *Klebsiella pneumoniae*, consists of evolutionarily conserved enzymes from the methionine salvage pathway, which recycles the γ-thiomethyl of methylthioadenosine to methionine [7–13]. Methylthioadenosine is both a product and a potent down-regulator of polyamine biosynthesis [14]. ARD catalyzes the penultimate step in the pathway, the oxidative decomposition of 1,2-dihydoxy-3-keto-5-(thiomethyl)pent-1-ene (aci-reductone) to formate and 2-keto-4-(thiomethyl)butyrate, the keto-acid precursor of methionine. This activity requires the enzyme to bind metal, and the products formed depend on which metal is bound. In bacterial enzymes, the association of ARD with Ni^{2+} results in ARD-mediated production of carbon monoxide, formate, and methylthiopropionate, whereas association with Fe^{2+} results in ARD′-mediated production of formate and the

Abbreviations: ARD, aci-reductone dioxygenase; *ADI1*, aci-reductone dioxygenase 1; BPH, benign prostatic hyperplasia; CHX, cycloheximide; DIG, digoxygenin; FBS, fetal bovine serum; GFP, green fluorescent protein; Mib, mibolerone; MT1-MMP, membrane type I matrix metalloproteinase; MTCBP-1, MT1-MMP cytoplasmic tail–binding protein-1; SDS, sodium dodecyl sulfate

Address all correspondence to: Zhou Wang, PhD, Department of Urology, University of Pittsburgh School of Medicine, Suite G40, 5200 Center Avenue, Pittsburgh, PA 15232.
E-mail: wangz2@upmc.edu

[1]This work was supported, in part, by NIH R01 DK51193 (Z.W.), NIH P50 CA90386 Prostate Cancer SPORE (Z.W.), and R01 GM067786 (T.C.P).
[2]Junkui Ai and Gina M. Pagani contributed equally to this work.
[3]Junkui Ai is an AUA Foundation postdoctoral fellow.
Received 15 May 2007; Revised 22 June 2007; Accepted 23 June 2007.

DOI 10.1593/neo.07415

keto-acid precursor to methionine [8,9,15]. Nuclear magnetic resonance–derived solution structures of the *Klebsiella* enzyme and the crystallographic structure of the ARD ortholog from *Mus musculus* have identified key histidine and glutamic acid residues within a conserved domain responsible for metal binding [9,13,16].

Evidence suggests a possible role for aci-reductone dioxygenase 1 (*ADI1*) in prostate cancer. We observed a downregulation of *ADI1* in rat and human prostate cancer cell lines. Moreover, enforced expression of rat *Adi1* in these prostate cancer cells induced apoptosis, suggesting that *ADI1* may have an inhibitory role in prostate cancer [7]. Through a yeast two-hybrid screen, Uekita et al. independently identified human *ADI1*. Using the cytoplasmic tail of membrane type I matrix metalloproteinase (MT1-MMP) as bait yielded MT1-MMP cytoplasmic tail–binding protein-1 (MTCBP-1) as a potential binding partner [17]. Sequence comparison characterized MTCBP-1 as an ortholog of rat *Adi1*. Transient expression of human *ADI1* in fibroblast cell lines inhibited MT1-MMP–mediated migration and Matrigel invasion [17]. Similar to prostate cancer cells, cultured gastric carcinoma cells and fibrosarcoma cells also have downregulated *ADI1* [7,17], consistent with an inhibitory role in tumor progression. However, it remains unknown whether *ADI1* expression also undergoes downregulation in human cancer specimens.

Recent work has demonstrated the ability of human *ADI1* to function in methionine metabolism in yeast. *Saccharomyces cerevisiae* can grow under sulfur-depleted conditions, using the methionine salvage pathway to regenerate methionine. Disruption of the yeast homolog of ARD *YMR009w* blocks this growth, which *ADI1* expression restores. This indicates that ADI1 is functionally conserved and can act as an ARD in yeast [18]. However, biochemical evidence for human ADI1 as an ARD enzyme is still lacking. In addition, it is unknown whether the enzymatic activity of ADI1 is required for its observed proapoptic activity in prostate cancer cells.

In this study, we further explore the expression and enzymatic activity of ADI1 in prostate cancer. We show the androgen regulation of human *ADI1* expression in prostate cancer cells and the downregulation of its expression in human prostate cancer specimens, further supporting a role for *ADI1* in prostate cancer progression. We also provide biochemical evidence that ADI1 can truly act as an ARD enzyme. Surprisingly, point mutations that disrupt the predicted metal-binding site essential for ADI1 enzymatic activity did not affect the ability of the protein to induce apoptosis and to suppress colony formation in prostate cancer cells, suggesting that these activities may be independent of ARD enzymatic activity.

Materials and Methods

Cloning of Human ADI1 cDNA and Construction of ADI1 Mutants

A full-length cDNA clone encoding human *ADI1* was isolated from a λZAP phage cDNA library and was prepared using LNCaP mRNA (Stratagene, La Jolla, CA). Rat *ADI1* cDNA was used as a probe using low-stringency conditions. *In vivo* excision of the λZAP phage yielded a pBluescript II SK plasmid (Stratagene, La Jolla, CA), with human *ADI1* cDNA inserted at the *Eco*RI and *Xho*I sites between T3 and T7 promoters. Nested deletion mutants were generated using the Erase-a-Base kit (Promega, Madison, WI) and then sequenced using the Alpha Express automated sequencing machine (Amersham Pharmacia, Piscataway, NJ). Both strands of cDNA were sequenced completely. Sequence assembly and analysis were carried out using the DNASIS program (Hitachi Software, San Francisco, CA).

The Quickchange Site-Directed Mutagenesis kit (Stratagene) was used to make *ADI1* mutants: *H1* (His88Ala), *H2* (His90Ala), *H3* (His133Ala), *E1* (Glu94Ala), *H1H2* (His88Ala and His90Ala), *H1H2E1* (His88Ala, His90Ala, and Glu94Ala), and *H1H2H3E1* (His88Ala, His90Ala, His133Ala, and Glu94Ala). In each case, histidine or glutamic acid was converted to an alanine, and all mutants were sequenced to confirm the mutation.

In Situ *Hybridization*

Sense and antisense *ADI1* RNA probes labeled with digoxygenin (DIG) were used for *in situ* hybridization studies. A full-length ADI1 cDNA inserted at the multiple cloning site of the pBluescript II SK plasmid was used in template preparation. Linearized proteinase K–treated plasmid DNA templates were prepared as described previously [19,20], and the synthesis of sense and antisense RNA probes was carried out by *in vitro* transcription using a DIG RNA labeling mix of nucleotides (Roche Molecular Biochemicals, Indianapolis, IN) with either T3 or T7 RNA polymerase (Promega). *In situ* hybridization was carried out according to the method of Furlow et al. [20] with minor modifications, as described in Cyriac et al. [19].

Tissue Array and Immunohistochemistry

Human radical prostatectomy specimens were obtained with consent and constructed into tissue microarrays (Northwestern University Urology Department and Pathology Core Facility). Each tissue core was evaluated and given a diagnosis by a genitourinary pathologist. Immunohistochemistry staining of tissue cores using purified antibodies (anti-ADI1 polyclonal antibody) [7] was performed at the Northwestern Pathology Core Facility. Two observers independently isolated the area of pathological diagnosis within the tissue core and scored the intensity of immunostaining using subjective Grizzle scores (1–4, with 4 = *the highest level of intensity*) [21]. If the scoring discrepancy between the two observers was $\geq$ 1.5, the tissue core was discarded from analysis. An average Grizzle score for each type of prostatic histology was then determined.

Cell Culture

LNCaP and PC3 prostate cancer cells were obtained from the American Type Culture Collection (Manassas, VA) and maintained in RPMI 1640 supplemented with 10% fetal bovine serum (FBS), 1% glutamine, and 1% penicillin–streptomycin at 37°C in a humidified atmosphere containing

5% CO_2. LNCaP cells were cultured in phenol red–free RPMI 1640 plus 10% charcoal-stripped FBS (cFBS) for 2 days before treatment with a synthetic androgen, Mibolerone (Mib; NEN Life Science Products, Boston, MA). For time-course studies, cells were treated with 1 nM Mib for indicated hours. To determine whether *ADI1* is a direct androgen-responsive gene, LNCaP cells were treated with cycloheximide (CHX; Sigma, St. Louis, MO) at 10 μg/ml for 2 hours before treatment with 1 nM Mib for 24 hours.

Western Blot Analysis

Cells were collected at indicated time points and lysed in a 1% sodium dodecyl sulfate (SDS) lysis buffer. Protein concentrations of cell lysates were determined using a Bio-Rad DC protein assay kit (Bio-Rad, Hercules, CA) and 30 μg of proteins loaded per well. Proteins were separated by SDS polyacrylamide gel electrophoresis (PAGE) and transferred to nitrocellulose, and Western blot analysis was performed as previously described [7]. The ADI1 polyclonal antibody, generated using a human ADI1 peptide sequence and affinity purification, has been previously shown to react strongly against human ADI1 [7]. Blots were incubated with ADI1 antibodies. After incubation with secondary antibodies linked to horseradish peroxidase, proteins were visualized by enhanced chemiluminescence. β-Actin was probed using antibodies obtained from Santa Cruz Biotechnology (Santa Cruz, CA).

Total RNA Isolation and Northern Blot Analysis

Total RNA was isolated from LNCaP cells using the RNeasy mini kit (Qiagen, Germantown, MD). Total RNA (10 μg) was electrophoresed through a 1% agarose formaldehyde gel, transferred to a nylon membrane, and then cross-linked to the membrane by UV irradiation. The transferred membrane and the premade multiple tissue Northern blot analyses purchased from Clontech (Palo Alto, CA) were hybridized overnight with a human *ADI1* cDNA probe labeled by random priming with α-[^{32}P]dCTP at 42°C in a solution containing 5× sodium chloride sodium phosphate EDTA, 2× Denhardt's solution, 0.1% SDS, 100 μg/ml denatured salmon sperm DNA, and 50% formamide. The membrane was then washed at room temperature with 1× saline sodium citrate (SSC) and 0.1% SDS for 20 minutes followed by three 20-minute washes at 65°C with 0.2× SSC and 0.1% SDS, and then exposed to X-ray film with an intensifying screen at −80°C.

Subcellular Localization and Apoptosis Assay

The coding region for human wild-type and mutant *ADI1* was cloned into the pEGFP-C1 vector (Clontech) at the *Eco*RI and *Kpn*I sites within the multiple cloning site (MCS), creating green fluorescent protein (GFP) fusion proteins at the N-terminus. Constructs were confirmed by restriction digestion and sequence verification as correct. Plasmid DNA for transient transfection were prepared using double-CsCl gradient banding.

Transient transfection for cell death genes has been described in Miura and Yuan [22]. Ten thousand PC3 cells were plated per well on six-well plates (for quantitation of apoptosis) or on coverslips (for subcellular localization), and transfections were carried out 24 hours later. pEGFP-C1, pEGFP-C1 + *ADI1*, or vectors were transfected into PC3 cells by FuGene transfection reagent (Roche, Basel, Switzerland). Transfections were carried out using a 6:1 transfection reagent/DNA ratio (1 μg/well DNA). At 24 hours posttransfection, cover slips were washed in phosphate-buffered saline (PBS), fixed in 3.7% formaldehyde solution for 10 minutes, washed thrice in PBS, transferred, and then sealed to microscope slides using Vectashield (Vector Laboratories, Burlingame, CA). The slides were viewed and pictures were taken on a Laser Scanning Confocal Microscope (LSM510; Zeiss, Jena, Germany) at the Cell Imaging Facility of Northwestern University. Quantitation of apoptosis was performed as previously described [7].

Colony Formation Assay

LNCaP cells, at 80% confluence in six-well plates, were transfected with GFP-tagged *ADI1*, GFP-tagged *ADI1* mutants, or empty vector pEGFP-C1 using Lipofectamine2000 (Invitrogen, Carlsbad, CA) at the same ratio used for PC3 cells. After 24 hours, all cells in each well were reseeded onto 10-cm tissue culture dishes with a medium containing G418 (500 μg/ml; Invitrogen) and then cultured for 3 weeks to allow colonies to develop. The medium was replaced weekly. All colonies larger than 1 mm in diameter were counted, and the number of GFP-positive colonies was noted. Each colony formation assay was carried out in triplicate and repeated at least thrice. All data obtained from colony formation assays were analyzed using GraphPad Prism (GraphPad Software, Inc., San Diego, CA). The statistical significance of differences in data was calculated using Tukey's Multiple Comparison Test.

ADI1 Protein Expression and Enzyme Activity Assay

Escherichia coli BL21 (DE3) cells were transformed with empty pET28a vector or pET28a containing the coding sequence of the human *ADI1* gene (pET-ADI1). Cultures were grown in Luria-Bertani broth with kanamycin (10 mg/ml) up to an OD_{600} of 0.6, at which point protein expression was induced with 0.5 mM isopropylthiogalactoside (IPTG). Induced cultures were grown for 3.5 hours and then resuspended in 30 mM potassium phosphate buffer, pH 7.5 (1:4, wt/vol). Cells were lysed by sonication, and insoluble fraction removed by centrifugation. The concentration of protein in the soluble fraction was determined with Bradford reagent (Bio-Rad). Lysates were separated on 15% SDS polyacrylamide gels and stained by Coomassie blue or transferred to nitrocellulose membrane for Western blot analysis, using anti-ADI1 antibodies as described previously [7].

ADI1 protein activity was tested against the substrate analog, 3-keto-1,2-dihydroxyhex-1-ene (aci-reductone). Aci-reductone was prepared by anaerobically incubating 60 μM 2,3-diketo-1-phosphohexane with purified recombinant *E1* enolase/phosphatase in 20 mM HEPES (pH 7.5) and 5 mM $MgCl_2$ with 10 μg/ml catalase [23]. Aci-reductone production was monitored by the increase in absorbance at 305 nm ($E_{305\ nm}$ = 20,000 M^{-1} cm^{-1}) on a Hewlett Packard 8452

photodiode array spectrophotometer (Hewlett Packard Co., Houston, TX). When no further increase in aci-reductone levels was observed, soluble cell lysate was added aerobically, and the decay of the substrate was monitored by following the changes in absorbance at 305 nm. Progress curves appeared to have two phases and were best described with a double exponential decay equation (SigmaPlot; Systat Software, Inc., San Jose, CA). The rate constant for the fast phase was used to calculate the specific activity of cellular extract.

Results

Structure and Sequence of the Human ADI1 Gene

A National Center for Biotechnology Information database search revealed that the human *ADI1* gene is located on the short arm of chromosome 2 at 2p25.3. The human *ADI1* gene consists of four exons that encode a predicted protein of 179 amino acids (Figure 1). This protein displays high homology to the ARD/ARD′ domain (pfam entry 03079) initially described in bacterial protein [9]; ADI1 has a double-stranded β-helix domain that both characterizes members of the cupin superfamily [24] and contains the ARD active site [9]. Indeed, ADI1 possesses the three histidines (His88, His90, and His133) and the glutamic acid (Glu94) required for members of the ARD/ARD′ family to bind metal (Figure 1) [8,9,15,16,25].

ADI1 mRNA Is Expressed in a Variety of Human Tissues

The rat prostate expresses high levels of *ADI1* [7]. To test whether human prostate also expresses high levels of ADI1 mRNA, we probed two commercially available human tissue Northern blot membranes using *ADI1* cDNA as a probe. As expected, the human prostate expressed abundant levels of *ADI1* mRNA at the predicted size of 1.6 kb (Figure 2). In addition, multiple other tissues also expressed *ADI1* mRNA, with the liver, kidney, thyroid, and skeletal muscle having the highest levels, and with leukocytes and the brain having barely detectable levels.

ADI1 Is Expressed in Prostatic Epithelial Cells

The prostate consists of mainly two cell types: epithelial and stromal. *In situ* hybridization experiments were performed on human benign prostatic hyperplasia (BPH) tissues to localize *ADI1* mRNA expression in the human prostate. Figure 3*A* shows an expression of *ADI1* mRNA in epithelial cells, with little or no expression in stromal cells. This finding is consistent with a previous observation that the epithelial cells of the rat prostate specifically express *ADI1* as do LNCaP cells, which are of epithelial origin [7].

ADI1 Is Downregulated in High-Grade Prostate Tumors

To determine whether human prostate cancer tissues have altered *ADI1* expression, we performed immunohistochemistry with our polyclonal ADI1 antibodies on a tissue array of prostate tumors. We have previously demonstrated that the antibody, which is generated with a human ADI1 peptide and affinity purification, recognizes rat and human ADI1 [7]. Figure 3*B* shows ADI1 staining in a representative specimen containing both benign tissues and a Gleason grade 3 tumor; tumor cells had less ADI1 protein than the benign region. The ADI1 staining intensity in the prostate tissue array was scored from 1 to 4 using the Grizzle method, with 4 representing the highest intensity of staining [21]. Tumors displayed an obvious downregulation of ADI1 protein levels (Figure 3*C*), which is consistent with the downregulation of *ADI1* mRNA in prostate cancer cell lines [7].

Expression of ADI1 mRNA Is Regulated By Androgens in LNCaP Cells

We first identified *ADI1* as an androgen-responsive gene in the rat ventral prostate [7,26]. To determine whether androgen regulation of *ADI1* also occurs in humans, we used the androgen-sensitive human prostate cancer cell line LNCaP [27]. LNCaP cells were treated with 1 nM of the synthetic androgen Mib, and *ADI1* expression was determined by Northern blot analysis. Mib induces *ADI1* mRNA, with an increase in expression occurring within 24 hours of treatment (Figure 4*A*). Western blot analysis demonstrated that the increase in *ADI1* mRNA is accompanied by an increase in

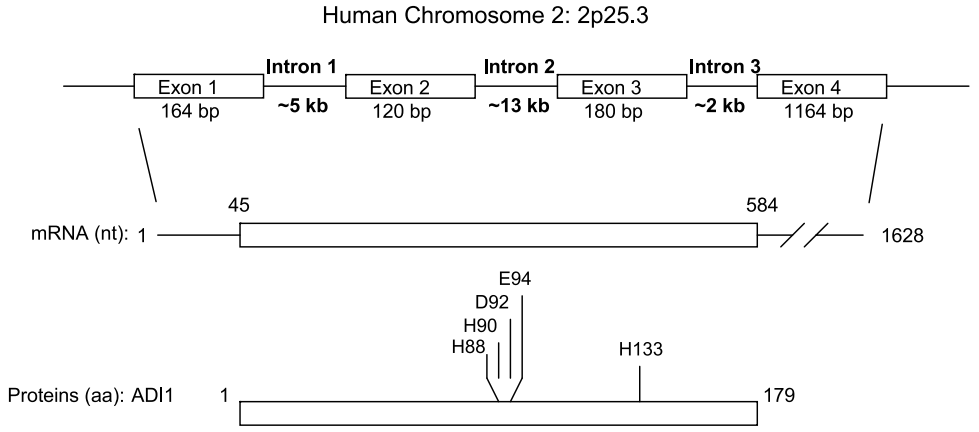

Figure 1. *Genomic structure of the human ADI1 gene. ADI1 is found in chromosome 2 at 2p25.3. The gene is encoded by four exons and has three introns.* ADI1 *protein consists of 179 amino acids, with the residues involved in binding Fe^{2+} or Ni^{2+}, His88, His90, His133, Asp92 (Fe^{2+}), and Glu94 (Ni^{2+}) [9,16] shown.*

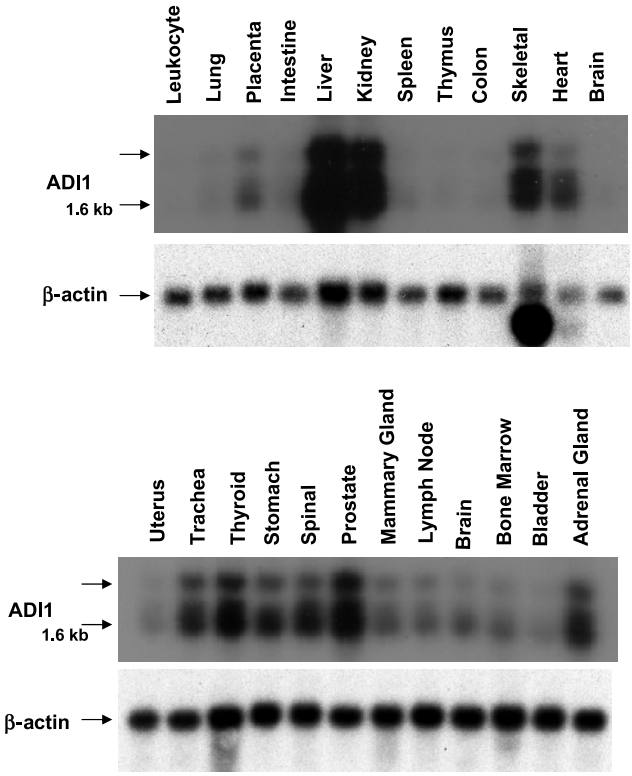

Figure 2. *Northern blot analysis of ADI1 expression in indicated human tissues. Northern blot filters contain polyA$^+$ RNA from indicated tissues and were purchased from Clontech. β-Actin served as the control for RNA loading levels.*

protein levels (Figure 4*B*). To determine whether *ADI1* is a primary androgen-responsive gene, we tested whether *ADI1* mRNA induction by Mib requires new protein synthesis. Figure 4*C* shows that the protein inhibitor CHX did not affect *ADI1* mRNA upregulation by Mib in LNCaP cells, indicating that androgens directly induce *ADI1*.

Enzymatic Activity Assay of Recombinant ADI1 Protein

ARD catalyzes the reaction between O_2 and the aci-reductone intermediate in the methionine salvage pathway. To determine whether human ADI1 protein has aci-reductone dioxygenase (ARD) activity, we expressed human *ADI1* in *E. coli* BL21 bacterial cells (Figure 5*A*). Aci-reductone was produced *in vitro* under anaerobic conditions [23], and the amount obtained was monitored spectroscopically. ARD activity was assayed by combining aci-reductone with bacterial lysates under aerobic conditions and by measuring the decay of aci-reductone at 305 nm. Lysates containing wild-type ADI1 exhibited at least a five-fold increase in ARD activity over endogenous activity (Table 1).

The ADI1 Metal-Binding Site Is Not Required for Apoptosis and Growth Inhibition

ARD enzymes require a metal cofactor for enzymatic activity [8,9,15]. Therefore, we tested the effect of mutating the amino acids likely required for metal binding on *ADI1* function in prostate cancer cells. We have previously demonstrated that rat *Adi1* induced prostate cancer cell death [7], so we measured apoptosis in PC3 cells expressing mutated *ADI1*. Seven *ADI1* point mutants were constructed by substituting alanine for residues expected to ligate the metal ion cofactor in the active site: *H1* (His88Ala), *H2* (His90Ala), *H3* (His133Ala), *E1* (Glu94Ala), *H1H3* (His88Ala and His133Ala), *H1H2E1* (His88Ala + His90Ala + Glu94Ala), and *H1H2H3E1* (His88Ala + His90Ala + His133Ala + Glu94Ala). In the bacterial ortholog of *ADI1*, mutating the corresponding residues to alanine eliminates both the ability of ADI1 to bind metal and its function as an ARD enzyme [13]. Single mutants of ADI1 were strongly expressed (Figure 5*B*), yet the specific activity of mutant lysates is less than that of lysates derived from BL21(DE3) cells containing an empty pET28 vector (Table 1). This observation suggests that overexpression of ADI1 protein suppresses endogenous bacterial enzymes: thus, mutations decrease the enzymatic activity of ADI1 by at least a factor of 50. Although double and triple mutants are poorly expressed, it is reasonable to expect that these variants would also be inactive.

To evaluate the subcellular location of the mutants, each was fused to GFP at its N-terminus. Fluorescent microscopy of PC3 cells 24 hours posttransfection revealed that wild-type ADI1 and the different mutants exhibited a similar

A

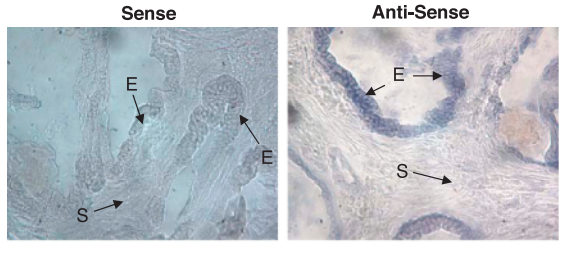

B

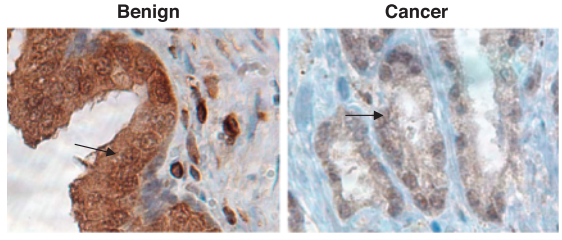

C

Staining Intensity	Benign(30)	Gleason Score 6(19)	7(16)	8(3)	9(4)
3 - 4.0	67%	5%	13%	33%	0
2 - 2.9	33%	53%	13%	0	0
1 - 1.9	0	42%	61%	67%	50%
0 - 0.9	0	0	13%	0	50%

Figure 3. *(A)* In situ *hybridization analysis of ADI1 mRNA in BPH tissue. Both antisense (right panel) and sense (left panel) ADI1 RNA probes were labeled with DIG and visualized with alkaline phosphatase–conjugated anti-DIG antibody. Epithelial (E) and stromal (S) cells are indicated by arrows. (B) Immunohistochemistry staining for* ADI1 *in the human prostate. Pictures show a representative benign prostate section and a Gleason 3 prostate tumor section in a single specimen stained with anti-*ADI1 *antibodies. Arrows indicate either benign or cancerous prostatic epithelial cells. (C) Quantitative analysis of the prostate cancer tissue array for* ADI1. *Staining intensity was adapted from Grizzle et al. [21], and Gleason scores were adapted from an independent pathologist (Northwestern Pathology Core Facilities). Numbers in parentheses indicate the number of samples.*

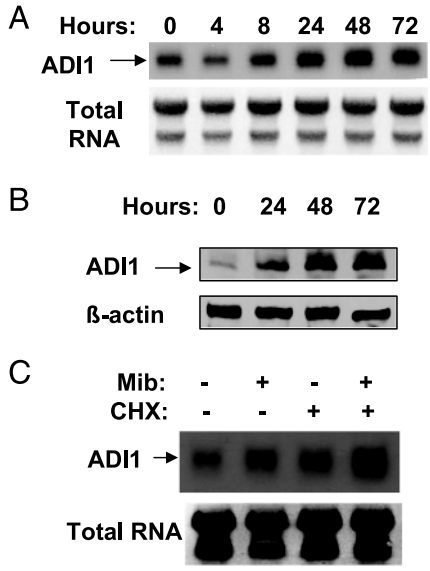

Figure 4. *(A) Northern blot analysis of the androgen regulation of ADI1 expression in LNCaP cells. LNCaP cells were grown in a medium containing 10% cFBS to remove all androgens. The total RNA harvested from LNCaP cells were treated with androgens (1 nM Mib) for indicated times.* ADI1 *mRNA is indicated by an arrow. (B) Western blot analysis of the androgen regulation of* ADI1 *protein expression. LNCaP cells were grown in RPMI 1640 medium containing 10% cFBS for 2 days to remove all androgens. Then cells were treated with 1 nM Mib, and cell lysates were collected at indicated time points.* ADI1 *protein is indicated by the arrow at 20 kDa, which is the predicted size. β-Actin served as the control for equal protein loading. (C) Northern blot analysis of the androgen regulation of ADI1 mRNA in the presence of CHX. Total RNA was harvested from androgen-deprived LNCaP cells and LNCaP cells treated with 1 nM Mib, 10 μg/ml CHX, or both. ADI1 mRNA is indicated by the arrow. The loading and the quality of total RNA in each lane were evaluated by staining the nylon membrane after transfer with methylene blue [39].*

localization, with fluorescence seen primarily in the perinuclear region in a punctate pattern (Figure 6*A*). Moreover, both wild-type and mutant ADI1 induced apoptosis, as indicated by altered Hoechst staining (Figure 6*A*). Quantitation of apoptosis in transfected cells, based on Hoechst staining, membrane blebbing, and cell detachment 48 hours post-transfection, demonstrated that mutant and wild-type proteins induced similar levels of cell death (Figure 6*B*). This suggests that metal binding and probably ARD enzymatic activity are not required for ADI1-induced apoptosis. Moreover, the use of transient transfection to introduce *ADI1* expression was only 10% efficient, with varying levels of proteins per cell (data not shown); yet, approximately 90% of transfected cells died. This argues that apoptosis is induced at various levels of ADI1 and that very little protein is required.

We also performed a colony formation assay using transfected LNCaP cells. After selection, only about 15% of the colonies transfected with the GFP-tagged wild-type *ADI1* expression vector were GFP-positive, whereas approximately 80% of the colonies transfected with GFP alone were GFP-positive (Figure 7), indicating that *ADI1* suppresses LNCaP colony formation. Interestingly, mutations in the predicted metal-binding site of *ADI1* did not affect its ability to inhibit colony formation. Decreased colony formation can be consistent with increased apoptosis; thus, this result may support our previous observation that ADI1-induced apoptosis does not require metal binding.

Discussion

ADI1 belongs to the family of ARD/ARD′ proteins that participate in the methionine salvage pathway [10–12]. These evolutionarily conserved enzymes can be found in organisms ranging from bacteria to humans. We have recently reported the induction of apoptosis by rat *Adi1* overexpression in transfected prostate cancer cell lines [7]. However, both the expression and the function of human *ADI1* in the prostate remain unknown. In this article, we report the down-regulation of *ADI1* in human prostate cancer specimens and the ability of human *ADI1* to induce apoptosis and to suppress colony formation in prostate cancer cells.

Similar to what we have observed in the rat prostate, androgens regulated human *ADI1* expression in LNCaP prostate cancer cells. Thus, androgen regulation of *ADI1* in the prostate is conserved between rats and humans. The protein synthesis inhibitor CHX did not inhibit androgen induction of

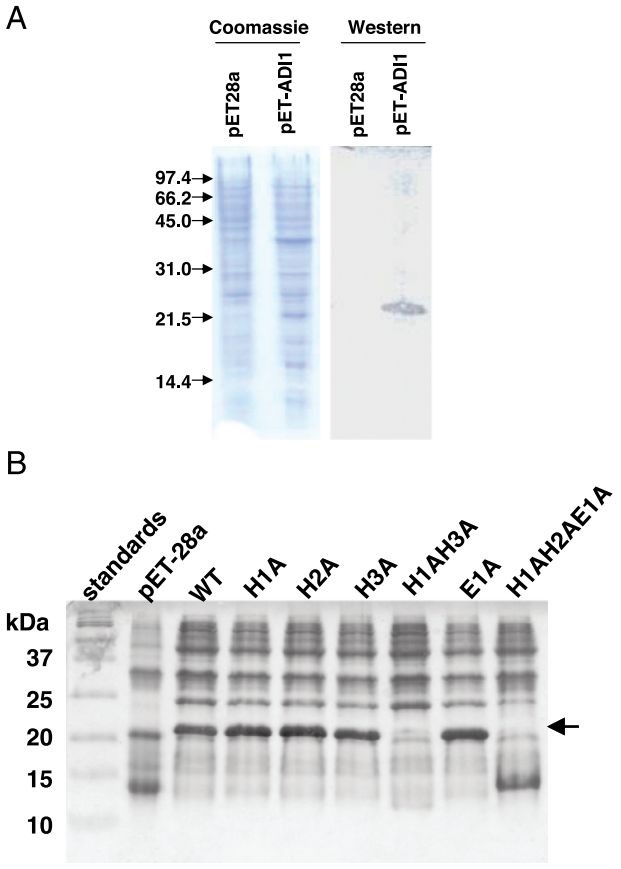

Figure 5. *(A) Expression of recombinant human* ADI1 *protein. The IPTG-induced expression of* ADI1 *protein in BL21 transformed with pET-ADI1 was detected by Western blot analysis using anti-*ADI1 *antibodies. BL21 transformed with pET28a was used as a control in parallel. The total* E. coli *lysates were visualized by Coomassie blue staining. Approximate molecular masses are indicated on the left (kDa).* ADI1 *protein has an expected molecular mass of 21,498 Da. (B) Coomassie-stained 15% SDS-PAGE of cell extracts expressing an empty vector or a vector containing ADI1. Empty vector and wild-type ADI1 are pET28a; mutant ADI1 constructs are expressed from pET23a. Approximate molecular masses are indicated on the left.*

Table 1. Specific Activities of Soluble Cell Extracts Containing Wild-Type and Mutant *ADI1* Constructs.

	Amount of Protein Assayed (mg)	k_{obs} (s^{-1})	Specific Activity (μmol/min per mg)
No lysate control	NA	0.005	NA
Empty pET-28a	4	0.01	8
Wild-type *ADI1*	11	0.14	39
H1A	13	0.02	0.5
H2A	16	0.03	0.7
H3A	14	0.02	0.5
E1A	16	0.02	0.4
H1AH3A	18	0.01	ND
H1AH2AE1A	12	0.02	ND
H1AH2AE1AH3A	9	0.02	ND

ADI1 activity was determined by monitoring the decrease in the absorbance of aci-reductone (λ_{max} = 305 nm) for 3 minutes. The protein content of cell extracts was determined by Bradford assay.
H1A, H88A; *H2A*, H90A; *H3A*, H133A; *E1A*, E94A; *ND*, not determined; *NA*, not applicable.
Specific activity is calculated by subtracting the background rate from k_{obs} and dividing by the amount of protein assayed.

ADI1, indicating that *ADI1* is a primary androgen-responsive gene. The ability of androgen to induce the expression of a growth-inhibitory gene is not surprising. Although androgen induces growth in a regressed prostate, it does not in a mature prostate. Instead, androgen maintains the homeostasis of a mature prostate and, in this context, induces the expression of growth-inhibitory genes. This balance becomes disrupted in prostate cancer. Given the importance of androgens in prostate cancer, this observation supports the possibility that *ADI1* plays a role in this disease.

The downregulation of ADI1 protein expression in human prostate cancer specimens argues that ADI1 potentially inhibits the growth that occurs during prostate cancer progression. This finding substantiates our previous observation that prostate cancer cell lines have downregulated *ADI1* expression. The human *ADI1* gene localizes to chromosome 2 at the 2p25.3 locus, a region that contains a potential novel tumor suppressor and is often lost in high-grade prostate tumors [28]. Introduction of this chromosomal region into the highly metastatic rat prostate cancer cell line AT6.1 significantly inhibited the metastasis of this tumor cell line in severe combined immunodeficient mice [28]. Because *ADI1* is inhibitory in prostate cancer, *ADI1* could be one of the genes responsible for metastasis suppression in this region.

Stable transfection of LNCaP cells with GFP-*ADI1* significantly inhibited the number of colonies formed compared with transfection with GFP alone. This finding is consistent with our previous observation that ADI1 is proapoptotic. In combination with downregulation of *ADI1* in human prostate cancer specimens, this observation strongly suggests an inhibitory role for *ADI1* in prostate cancer progression.

ADI1 shares homology with ARD enzymes, prompting the question of whether ADI1 possesses ARD activity. Northern blot analysis of *ADI1* expression in different human tissues shows that the highest levels of *ADI1* expression occur in the liver, kidney, and prostate. The liver is a major site for methionine salvage in the body [12], supporting the possibility that *ADI1* may function as an ARD enzyme. The prostate has one of the highest polyamine concentrations of any tissue [29,30]. The methionine salvage pathway recycles methylthioadenosine, an inhibitory byproduct of polyamine biosynthesis [31–34]; thus, a high-level expression of *ADI1* in the prostate may facilitate the necessary polyamine

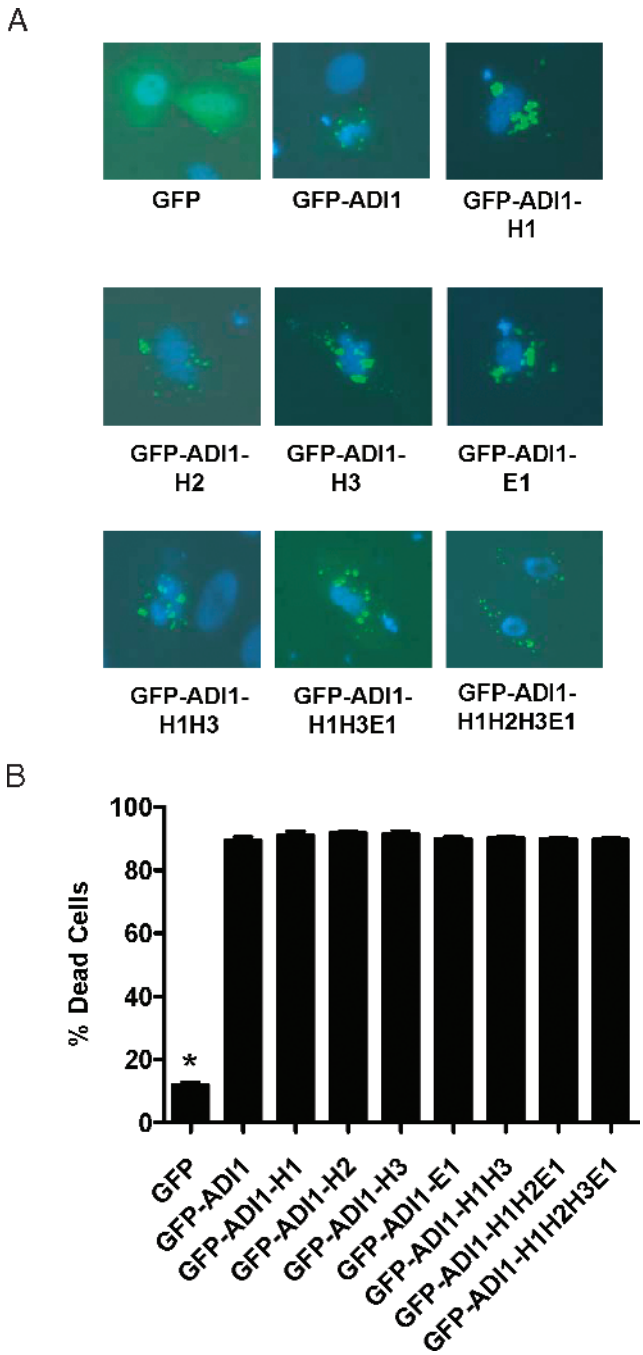

Figure 6. *(A) Subcellular localization of GFP-tagged wild-type and mutant ADI1 constructs in transiently transfected PC3 cells. Green fluorescent microscopy 24 hours posttransfection shows that* ADI1 *wild-type and mutant proteins have a similar subcellular localization. Hoechst staining revealed fragmented nuclei in cells transfected with GFP-tagged ADI1 or ADI1 mutants, but not in cells transfected with GFP only. (B) Percentage of dead PC3 cells 48 hours after transfection with GFP-ADI1 constructs. Dead* GFP*-positive cells were scored by fragmented nuclei and membrane blebbing.* ADI1 *mutant proteins had a similar ability to induce apoptosis in PC3 cells. The results represent the mean of three independent experiments, and error bars represent standard errors. *P < .001.*

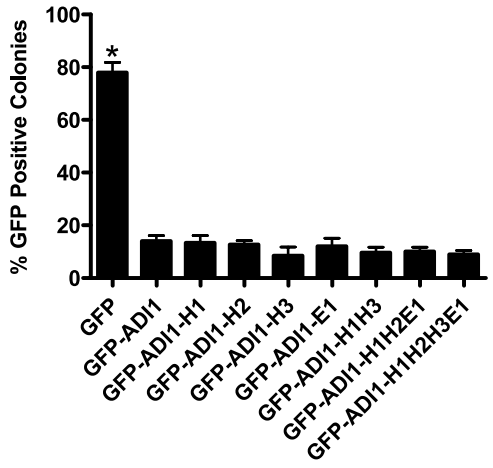

Figure 7. *Inhibition of LNCaP colony formation by GFP-tagged wild-type and mutant ADI1 constructs. The number of colonies with a diameter of ≥ 1 mm formed in monolayer culture was counted 3 weeks after drug selection. All GFP-ADI1 constructs inhibited colony formation (P < .001) relative to GFP control. No significant difference was observed between different GFP-ADI1 constructs. Each result is the mean of three independent experiments, and error bars represent standard errors. *P < .001.*

production. A potential role for ADI1 in the methionine salvage pathway is further supported by our finding that human ADI1 possesses enzymatic activity as an ARD in an *in vitro* assay.

Our experiments argue that the proapoptotic activity of ADI1 appears to be independent of its ARD enzymatic activity. The best-characterized role for the ARD/ARD′ family is its ability to act as an ARD, a function that requires metal binding [8,9,15]. There are four conserved amino acid residues (His88, His90, His133, and Glu94) that are critical for metal binding based on the structural analysis of these proteins [9,16]. Substitution of one, two, three, or four of these conserved amino acid residues did not affect the ability of ADI1 to induce apoptosis or to suppress the colony formation of prostate cancer cells, suggesting that ADI1 may mediate apoptosis through another mechanism. Indeed, ADI1 has been reported to have additional functions. ADI1 can bind to and inhibit the activity of MT1-MMP [17]. The alternative splice variant of ADI1, the protein Sip-L, consists of ADI1 amino acids 64 to 179 and can support hepatitis C virus replication in a nonpermissive cell line [35]. The yeast homologue of *ADI1*, *YMR009w*, encodes a potential binding protein of a splicing factor SNP-1, according to the comprehensive yeast protein–protein interaction database [36]. Future studies will be required to determine whether ADI1 induction of apoptosis in prostate cancer involves one of the above reported functions for ADI1 or a novel mechanism.

Microscopy revealed that GFP-ADI1 is found in a punctuate pattern that coincides with membrane ruffling and is near the perinuclear space. A similar punctuate subcellular localization was seen with V5 epitope-tagged Sip-L [35]. Hydrophobicity plots of ADI1 indicate that it is a very polar molecule (data not shown). Thus, we speculate that ADI1 may interact with polar head groups of the inner leaflet of the plasma membrane. Others have shown that ADI1 binds the cytoplasmic tail of MT1-MMP, inhibiting its activity [17]. This provides another explanation for the subcellular localization of ADI1. The colocalization of ADI1 and MTI-MMP would further suggest a role for ADI1 in prostate cancer, as MT1-MMP expression is upregulated in prostate tumors [37] and plays a role in enhancing migration through the cleavage of basement membrane proteins [38]. Our observation that ADI1 protein tagged with GFP at the C-terminus resulted in the same subcellular localization as protein tagged at the N-terminus (data not shown) indicates that GFP tag likely did not interfere.

In summary, our studies demonstrate the ability of human *ADI1*, whose expression is androgen-mediated, to induce apoptosis and to inhibit colony formation. Furthermore, we observed the downregulation of *ADI1* in human prostate cancer specimens. Together, these observations support an inhibitory role for *ADI1* in prostate cancer progression. Although ADI1 has ARD activity, the suppressive activity of ADI1 appears to be independent of this. Thus, a better understanding of prostate cancer progression will require further investigation of *ADI1* activity in prostate cells.

Acknowledgements

We thank the members of Wang laboratory for critical reading of this manuscript.

References

[1] Jemal A, Siegel R, Ward E, Murray T, Xu J, and Thun MJ (2007). Cancer statistics, 2007. *CA Cancer J Clin* **57**, 43–66.
[2] Bruchovsky N and Lesser B (1976). Control of proliferative growth in androgen responsive organs and neoplasms. *Adv Sex Horm Res* **2**, 1–55.
[3] Huggins C (1967). Endocrine-induced regression of cancers. *Cancer Res* **27**, 1925–1930.
[4] Kozlowski J and Grayhack J (1991). Carcinoma of the Prostate, 2nd ed, Chicago: Mosby Year Book, p1277–1393.
[5] Jiang F and Wang Z (2003). Identification of androgen-responsive genes in the rat ventral prostate by complementary deoxyribonucleic acid subtraction and microarray. *Endocrinology* **144**, 1257–1265.
[6] Zhou Z, Wong C, Sar M, and Wilson E (1994). The androgen receptor: an overview. *Recent Prog Horm Res* **49**, 249–274.
[7] Oram S, Jiang F, Cai X, Haleem R, Dincer Z, and Wang Z (2004). Identification and characterization of an androgen-responsive gene encoding an aci-reductone dioxygenase-like protein in the rat prostate. *Endocrinology* **145**, 1933–1942.
[8] Dai Y, Pochapsky TC, and Abeles RH (2001). Mechanistic studies of two dioxygenases in the methionine salvage pathway of *Klebsiella pneumoniae*. *Biochemistry* **40**, 6379–6387.
[9] Pochapsky TC, Pochapsky SS, Ju T, Mo H, Al-Mjeni F, and Maroney MJ (2002). Modeling and experiment yields the structure of acireductone dioxygenase from *Klebsiella pneumoniae*. *Nat Struct Biol* **9**, 966–972.
[10] Myers RW, Wray JW, Fish S, and Abeles RH (1993). Purification and characterization of an enzyme involved in oxidative carbon–carbon bond cleavage reactions in the methionine salvage pathway of *Klebsiella pneumoniae*. *J Biol Chem* **268**, 24785–24791.
[11] Wray JW and Abeles RH (1993). A bacterial enzyme that catalyzes formation of carbon monoxide. *J Biol Chem* **268**, 21466–21469.
[12] Wray JW and Abeles RH (1995). The methionine salvage pathway in *Klebsiella pneumoniae* and rat liver. Identification and characterization of two novel dioxygenases. *J Biol Chem* **270**, 3147–3153.
[13] Pochapsky TC, Pochapsky SS, Ju T, Hoefler C, and Liang J (2006). A refined model for the structure of acireductone dioxygenase from *Klebsiella* ATCC 8724 incorporating residual dipolar couplings. *J Biomol NMR* **34**, 117–127.
[14] Avila MA, Garcia-Trevijano ER, Lu SC, Corrales FJ, and Mato JM (2004). Methylthioadenosine. *Int J Biochem Cell Biol* **36**, 2125–2130.
[15] Dai Y, Wensink PC, and Abeles RH (1999). One protein, two enzymes. *J Biol Chem* **274**, 1193–1195.
[16] Xu Q, Schwarzenbacher R, Krishna SS, McMullan D, Agarwalla S,

Bowden GT, Abdubek P, Ambing E, Axelrod H, Biorac T, et al. (2006). Crystal structure of acireductone dioxygenase (ARD) from *Mus musculus* at 2.06 angstrom resolution. *Proteins* **64**, 808–813.

[17] Uekita T, Gotoh I, Kinoshita T, Itoh Y, Sato H, Shiomi T, Okada Y, and Seiki M (2004). Membrane-type 1 matrix metalloproteinase cytoplasmic tail–binding protein-1 is a new member of the Cupin superfamily: a possible multifunctional protein acting as an invasion suppressor down-regulated in tumors. *J Biol Chem* **279**, 12734–12743.

[18] Hirano W, Gotoh I, Uekita T, and Seiki M (2005). Membrane-type 1 matrix metalloproteinase cytoplasmic tail binding protein-1 (MTCBP-1) acts as an eukaryotic aci-reductone dioxygenase (ARD) in the methionine salvage pathway. *Genes Cells* **10**, 565–574.

[19] Cyriac J, Haleem R, Cai X, and Wang Z (2002). Androgen regulation of spermidine synthase expression in the rat prostate. *Prostate* **50**, 252–261.

[20] Furlow JD, Berry DL, Wang Z, and Brown DD (1997). A set of novel tadpole specific genes expressed only in the epidermis are down-regulated by thyroid hormone during *Xenopus laevis* metamorphosis. *Dev Biol* **182**, 284–298.

[21] Grizzle WE, Myers RB, Manna U, and Srivastava S (1998). Immunohistochemical evaluation of biomarkers in prostatic and colorectal neoplasia: Tumor Marker Protocols: Methods in Molecular Medicine. M Hanausek and Z Walaszek (Eds). Humana Press, Totowa, NJ.

[22] Miura M and Yuan J (2000). Transient transfection assay of cell death genes. *Methods Enzymol* **322**, 480–492.

[23] Zhang Y, Heinsen MH, Kostic M, Pagani GM, Riera TV, Perovic I, Hedstrom L, Snider BB, and Pochapsky TC (2004). Analogs of 1-phosphonooxy-2,2-dihydroxy-3-oxo-5-(methylthio)pentane, an acyclic intermediate in the methionine salvage pathway: a new preparation and characterization of activity with *E1* enolase/phosphatase from *Klebsiella oxytoca*. *Bioorg Med Chem* **12**, 3847–3855.

[24] Dunwell JM, Culham A, Carter CE, Sosa-Aguirre CR, and Goodenough PW (2001). Evolution of functional diversity in the cupin superfamily. *Trends Biochem Sci* **26**, 740–746.

[25] Ju T, Goldsmith RB, Chai SC, Maroney MJ, Pochapsky SS, and Pochapsky TC (2006). One protein, two enzymes revisited: a structural entropy switch interconverts the two isoforms of acireductone dioxygenase. *J Mol Biol* **363**, 823–834.

[26] Wang Z, Tufts R, Haleem R, and Cai X (1997). Genes regulated by androgen in the rat ventral prostate. *Proc Natl Acad Sci USA* **94**, 12999–13004.

[27] Horoszewicz JS, Leong SS, Kawinski E, Karr JP, Rosenthal H, Chu TM, Mirand EA, and Murphy GP (1983). LNCaP model of human prostatic carcinoma. *Cancer Res* **43**, 1809–1818.

[28] Mashimo T, Goodarzi G, Watabe M, Cuthbert AP, Newbold RF, Pai SK, Hirota S, Hosobe S, Miura K, Bandyopadhyay S, et al. (2000). Localization of a novel tumor metastasis suppressor region on the short arm of human chromosome 2. *Genes Chromosomes Cancer* **28**, 285–293.

[29] Schipper RG, Romijn JC, Cuijpers VM, and Verhofstad AA (2003). Polyamines and prostatic cancer. *Biochem Soc Trans* **31**, 375–380.

[30] Fjosne HE, Ostensen MA, Haarstad H, and Sunde A (1990). Androgen regulation of polyamine synthesis in seminal vesicle and in different lobes of the rat prostate. *Prostate* **17**, 1–11.

[31] Chattopadhyay MK, Tabor CW, and Tabor H (2005). Studies on the regulation of ornithine decarboxylase in yeast: effect of deletion in the *MEU1* gene. *Proc Natl Acad Sci USA* **102**, 16158–16163.

[32] Chattopadhyay MK, Tabor CW, and Tabor H (2006). Methylthioadenosine and polyamine biosynthesis in a *Saccharomyces cerevisiae* meu1-delta mutant. *Biochem Biophys Res Commun* **343**, 203–207.

[33] Yamanaka H, Kubota M, and Carson DA (1987). Synergistic inhibition of polyamine synthesis and growth by difluoromethylornithine plus methylthioadenosine in methylthioadenosine phosphorylase–deficient murine lymphoma cells. *Cancer Res* **47**, 1771–1774.

[34] Hibasami H, Borchardt RT, Chen SY, Coward JK, and Pegg AE (1980). Studies of inhibition of rat spermidine synthase and spermine synthase. *Biochem J* **187**, 419–428.

[35] Yeh CT, Lai HY, Chen TC, Chu CM, and Liaw YF (2001). Identification of a hepatic factor capable of supporting hepatitis C virus replication in a nonpermissive cell line. *J Virol* **75**, 11017–11024.

[36] Fromont-Racine M, Rain JC, and Legrain P (1997). Toward a functional analysis of the yeast genome through exhaustive two-hybrid screens. *Nat Genet* **16**, 277–282.

[37] Cardillo MR, Di Silverio F, and Gentile V (2006). Quantitative immunohistochemical and *in situ* hybridization analysis of metalloproteinases in prostate cancer. *Anticancer Res* **26**, 973–982.

[38] Bair EL, Chen ML, McDaniel K, Sekiguchi K, Cress AE, Nagle RB, and Bowden GT (2005). Membrane type 1 matrix metalloproteinase cleaves lamin-10 and promotes prostate cancer cell migration. *Neoplasia* **7**, 380–389.

[39] Herrin DL and Schmidt GW (1988). Rapid, reversible staining of Northern blots prior to hybridization. *Biotechniques* **6**, 196–197 (199–200).